Electronic Supplementary Information (ESI)

A nanotubular framework with customized conductivity and porosity for efficient oxidation and reduction of water

Jun Wu,[a, b] Lianwen Zhu,[*,b] Dan Deng,[c] Longfeng Zhu,[b] Li Gu[c] and Xuebo Cao[*,b]

[a] College of Chemistry, Chemical Engineering and Material Science, Soochow University, Suzhou, Jiangsu 215123, China

[b] School of Biology and Chemical Engineering, Jiaxing University, Jiaxing, Zhejiang 314001, China. E-mail: xbcao@mail.zjxu.edu.cn; lwzhu@mail.zjxu.edu.cn

[c] School of Materials and Textile Engineering, Jiaxing University, Jiaxing, Zhejiang, 314001, China

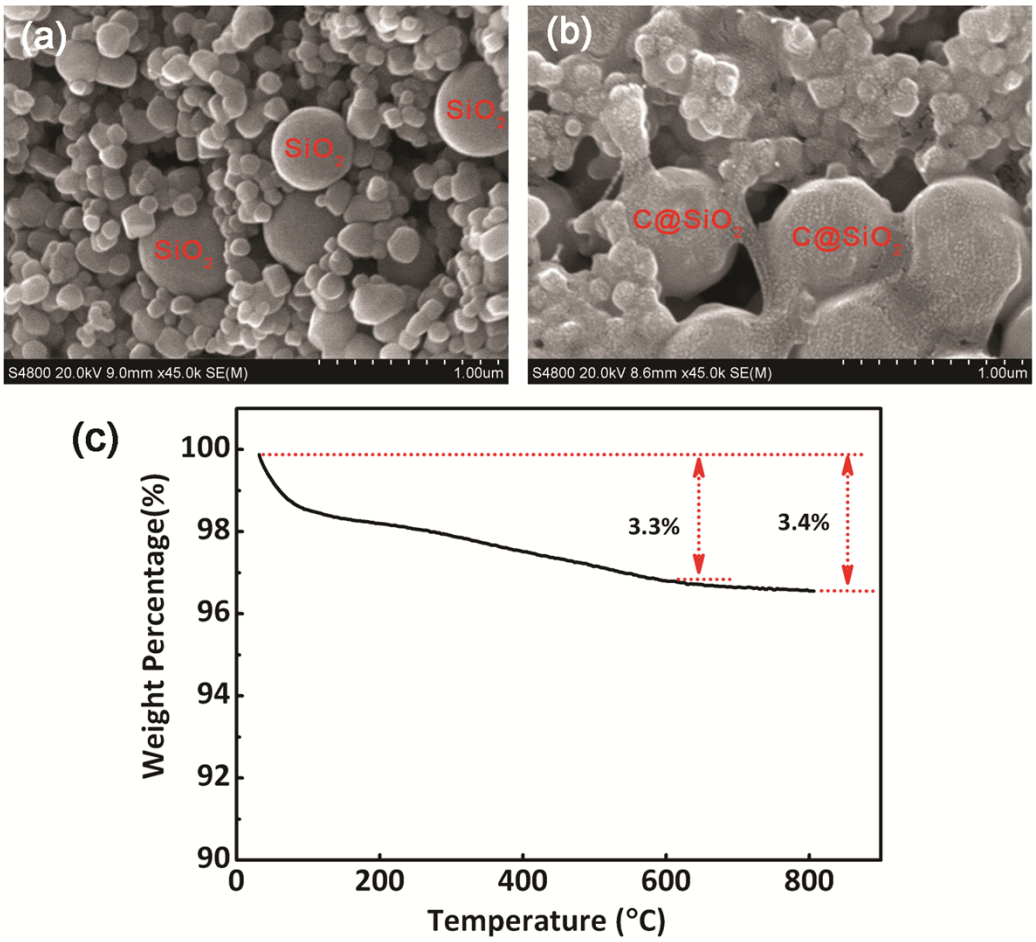

Fig. S1 (a) SEM image of TiO_2 nanoparticles and SiO_2 microspheres filled in Ni foam. (b) SEM image of TiO_2 nanoparticles and SiO_2 microspheres after the infiltration and pyrolysis of FFA. It is clearly seen that the surfaces of TiO_2 nanoparticles and SiO_2 microspheres are encapsulated by a layer of carbon. Upon the alkaline hydrothermal treatment of TiO_2 nanoparticles, carbon would coat on the converted TNTs. (c) TGA curve for Ni foam filled by TiO_2 nanoparticles, SiO_2 microspheres, and FFA. From the curve, it can be found that FFA is completely converted to carbon at 800 °C as there is little weight change at the temperature higher than 600 °C.

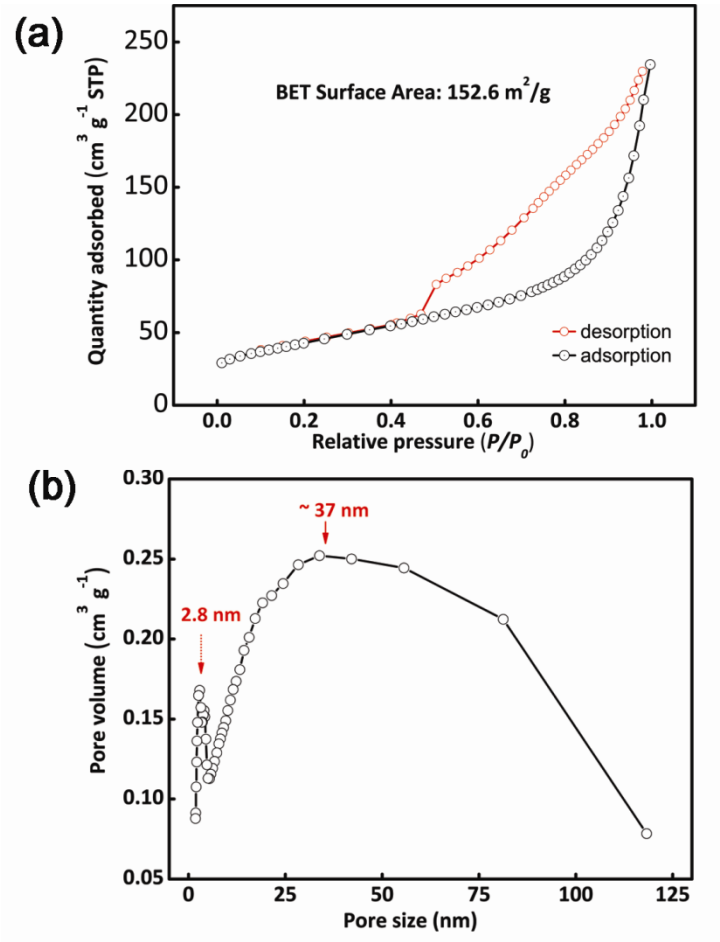

Fig. S2 (a) Nitrogen adsorption–desorption isotherms of Ni^x/C/TNTs framework at 77 K. The large hysteresis in the P/P_0 range of 0.4–1.0 indicates the presence of abundant mesopores. (b) BJH pore-size distribution plots determined from the desorption branch. The 2.8-nm pores correspond to the channels of the nanotubes, while the 37-nm pores are attributed to the interstices among the neighboring nanotubes.

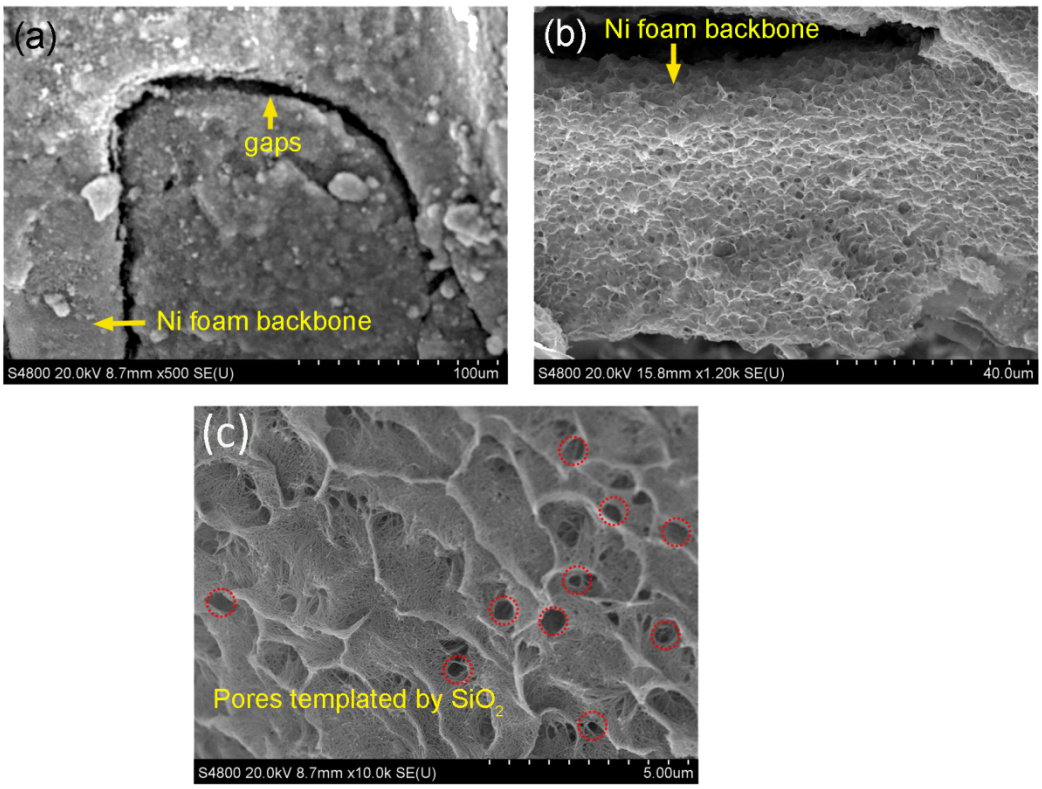

Fig. S3 (a) SEM image showing the gap between the Ni foam backbone and Ni^x/C/TNTs framework. The width of the gap is about 10 μm. (b) and (c) SEM images show that the backbone of Ni foam is also grown by Ni^x/C/TNTs framework, where the red circles indicate the presence of holes templated by SiO_2 microspheres.

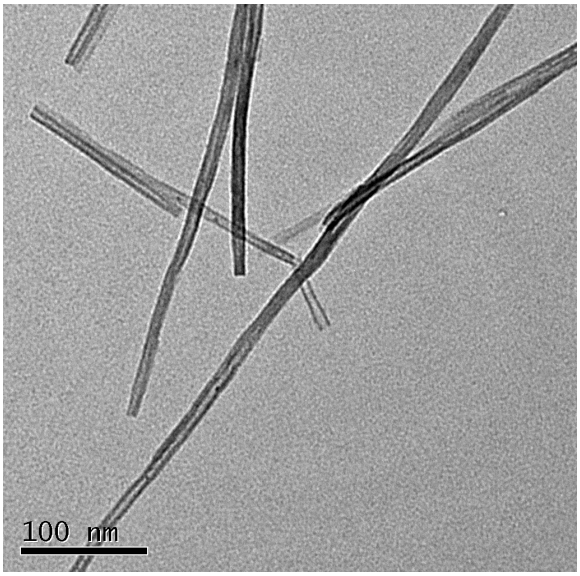

Fig. S4 TEM image of the pristine titanate nanotubes (TNTs). It clearly reveals that the surfaces of the pristine TNTs are clean.

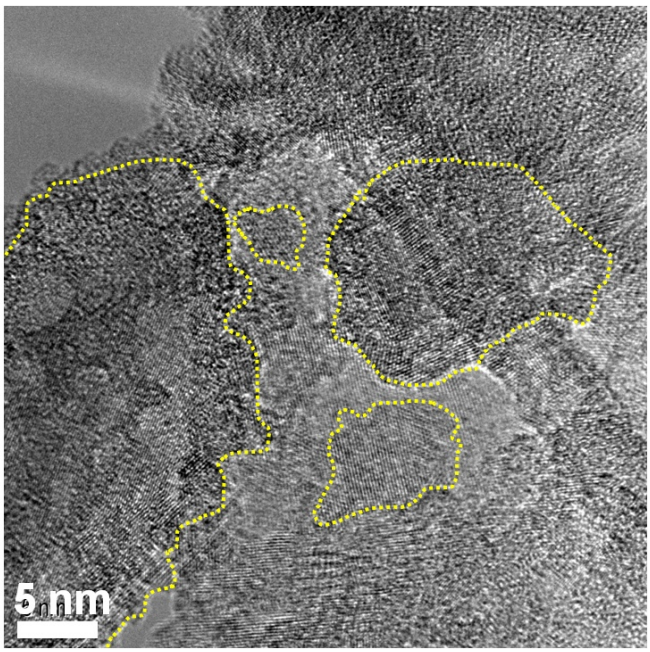

Fig. S5 Irregular fine crystallites (marked by the dot lines) are also observed in the TEM samples. They are found to belong to the hexagonal $Ni(OH)_2$ according to the XRD studies.

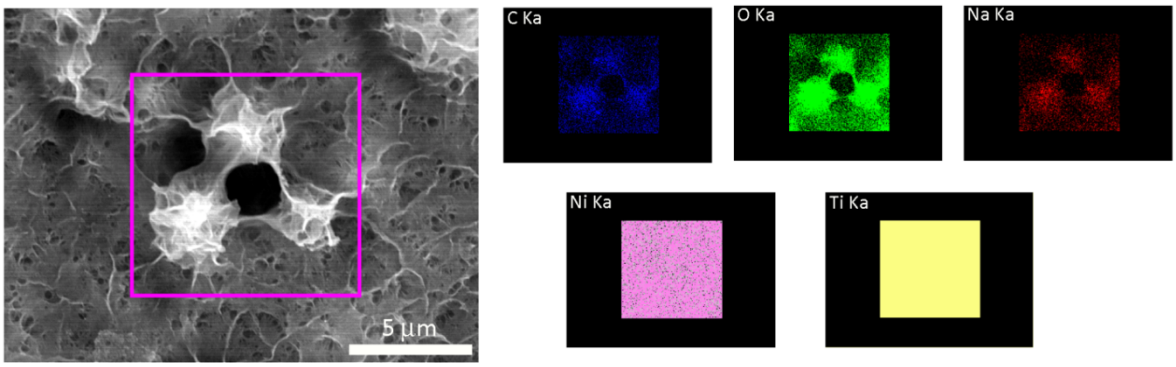

Fig. S6 Mapping measurements performed on the region marked by the square. The results demonstrate that the elements associated with Ni^x/C/TNTs framework (C, O, Na, Ni, and Ti) are homogeneously distributed in the sample. Owing to the relatively large atomic numbers, Ni and Ti can generate intense characteristic X-ray, thus leading to the shielding of the hole in the images of Ni ka and Ti ka.

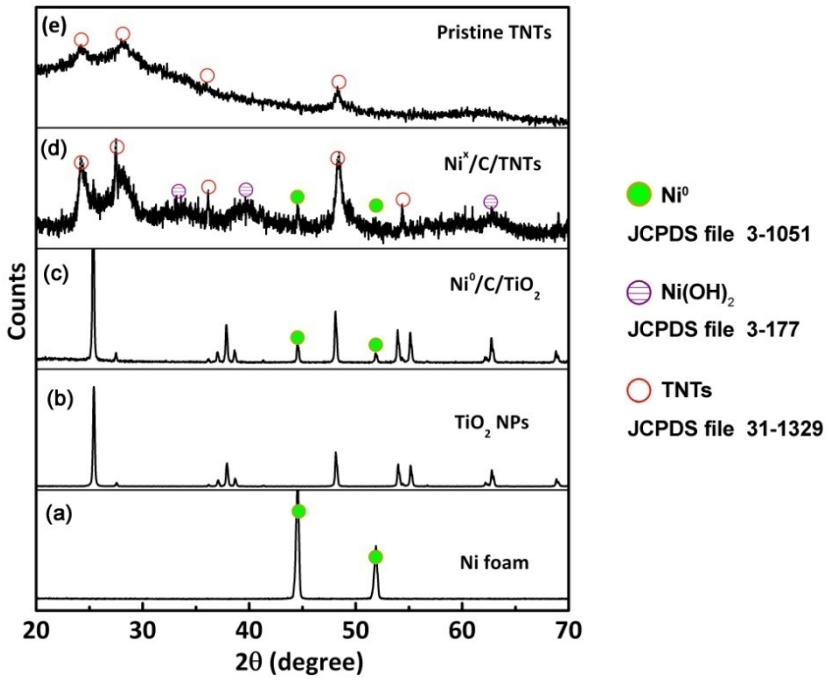

Fig. S7 XRD characterizations clarify the formation of Ni^0 and $Ni(OH)_2$ species. (a) Blank Ni foam. (b) TiO_2 nanoparticles for filling Ni foam. (c) The intermediate after the pyrolysis of FFA. (d) Ni^x/C/TNTs framework detached from the Ni foam. (e) Pristine TNTs. By comparing the XRD patterns of various samples, it can be found that Ni^0 and $Ni(OH)_2$species were detected at the stage of thermal annealing (Panel c) and at the stage of alkaline hydrothermal treatment (Panel d), respectively.

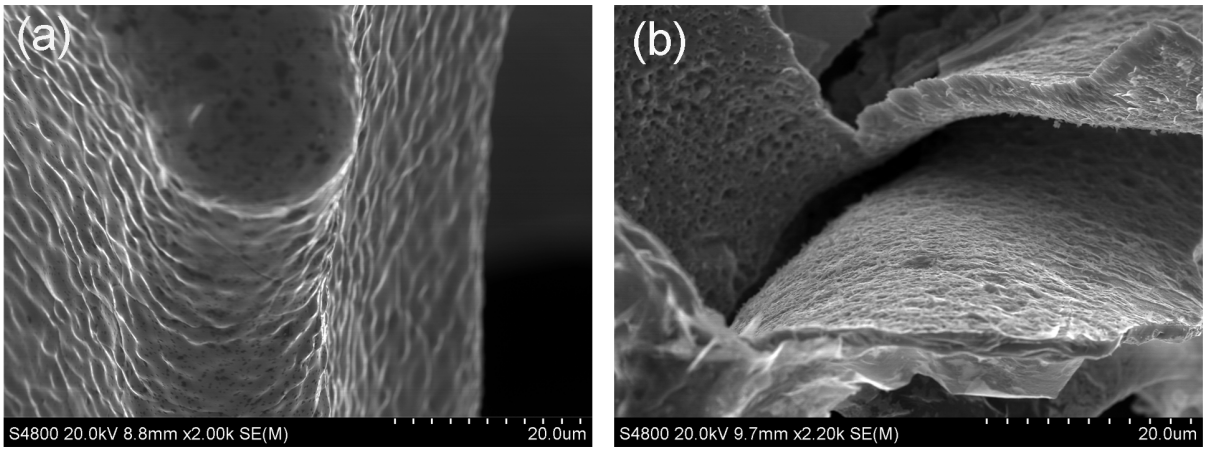

Fig. S8 (a) SEM image shows the backbone of Ni foam before loading TiO_2, SiO_2, and FFA. (b) SEM image shows the backbone of Ni foam after loading TiO_2, SiO_2, and FFA and the pyrolysis of FFA. It is clearly seen that exfoliation occurred, which is ascribed to the erosion of FFA, *p*–toluenesulfonic acid, and various pyrolysis products at the high temperature.

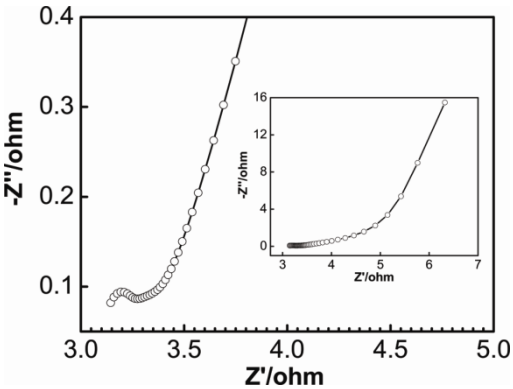

Fig. S9 Electrochemical impedance spectra of Ni^x/C/TNTs framework recorded under the following conditions: AC voltage amplitude 5 mV, frequency ranges 10^6 to 0.01 Hz, and open circuit (0.36 V versus RHE).

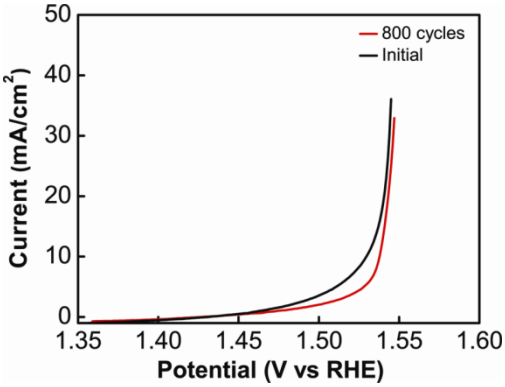

Fig. S10 Stability test of Ni^x/C/TNTs framework for OER. The polarization curve after 800 cycles is almost the same as the initial one.

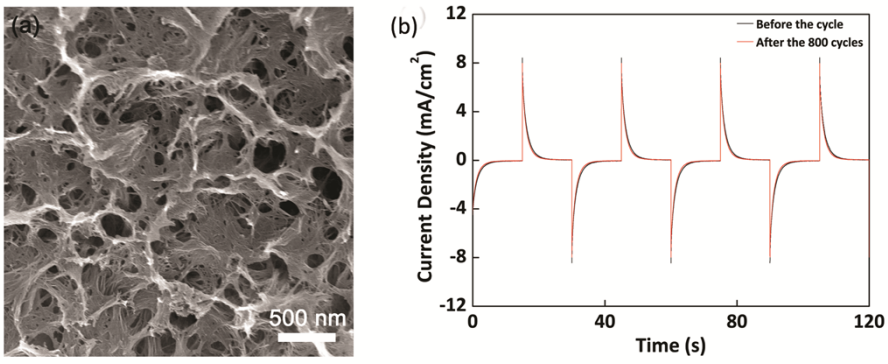

Fig. S11. (a) SEM image of the Ni^x/C/TNTs framework after the cycles. (b) *I* vs. *t* profiles for potential–step measurements of Ni^x/C/TNTs framework before (black line) and after (red line) the cycles.

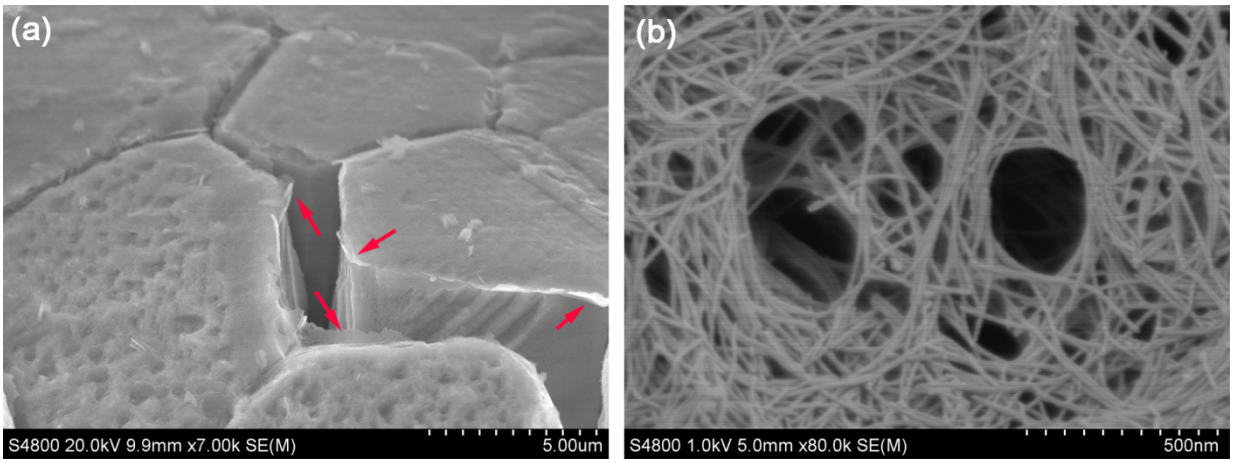

Fig. S12 In order to achieve in-depth understanding on the synergy of Ni^x, C, and TNTs within Ni^x/C/TNTs framework, we also synthesized the counterparts of Ni^x/C/TNTs framework, such as C-coated Ni foam and single TNTs framework supported by the Ni foam (free of carbon coating).

The sample of C-coated Ni foam was prepared as follows: firstly impregnating Ni foam in FFA, then annealing it at 800 °C, and last treating it in the alkaline hydrothermal environment at 140 °C. As shown in **Panel *a***, a layer of carbon film (denoted with arrows) is covered on the backbone of the Ni foam. Meanwhile, a number of cracks is the result of the thermal corrosion of the Ni foam by FFA, furthering verifying the growth mechanism of Ni^0 species in the Ni^x/C/TNTs framework.

The sample of single TNTs framework anchored on the Ni foam was prepared as follows: firstly filling Ni foam by TiO_2 nanoparticles and SiO_2 microspheres (W_{TiO2}:W_{SiO2}=2:1), then annealing it at 800 °C, and last treating it in the alkaline hydrothermal environment at 140 °C. as shown in the **Panel *b***, the titanate nanotubes also organize into the framework.

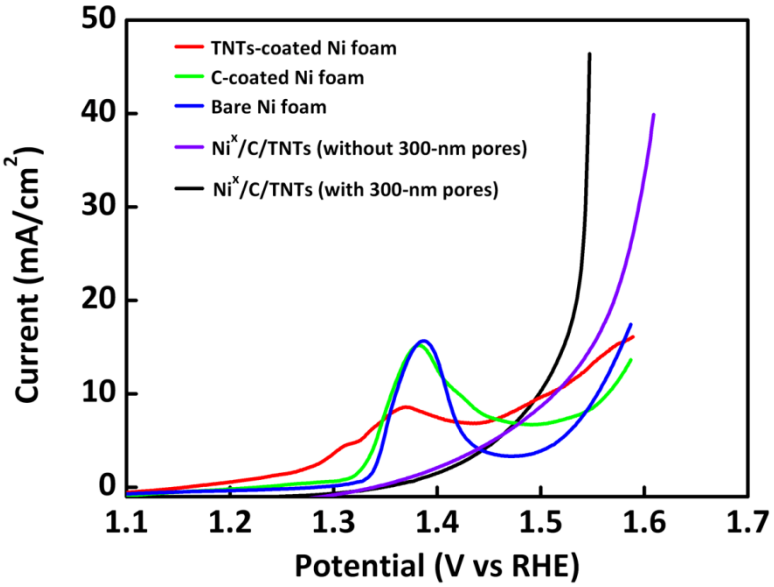

Fig. S13 A comparison among the OER performances of bare Ni foam (blue curve), C-coated Ni foam (green curve), single TNTs framework supported by the Ni foam (red curve), Ni^x/C/TNTs framework with the 300-nm pores (black curve), and Ni^x/C/TNTs framework without the 300-nm pores (violet curve).

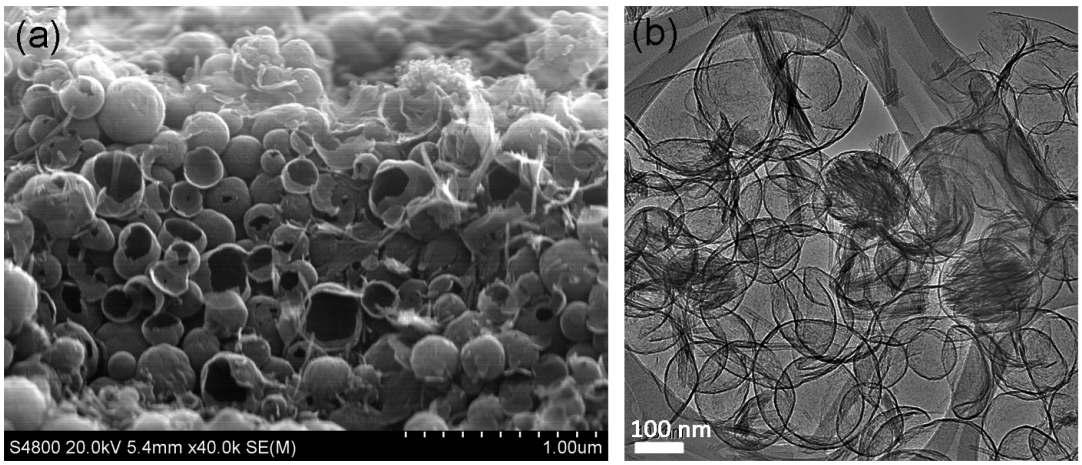

Fig. S14 (a) SEM measurement shows that there is a layer of dense spherical C covering the Ni foam backbone, which prevents the electrolyte to contact the Ni foam underlying Ni^x/C/TNTs framework and prevents the Ni foam from oxidation.

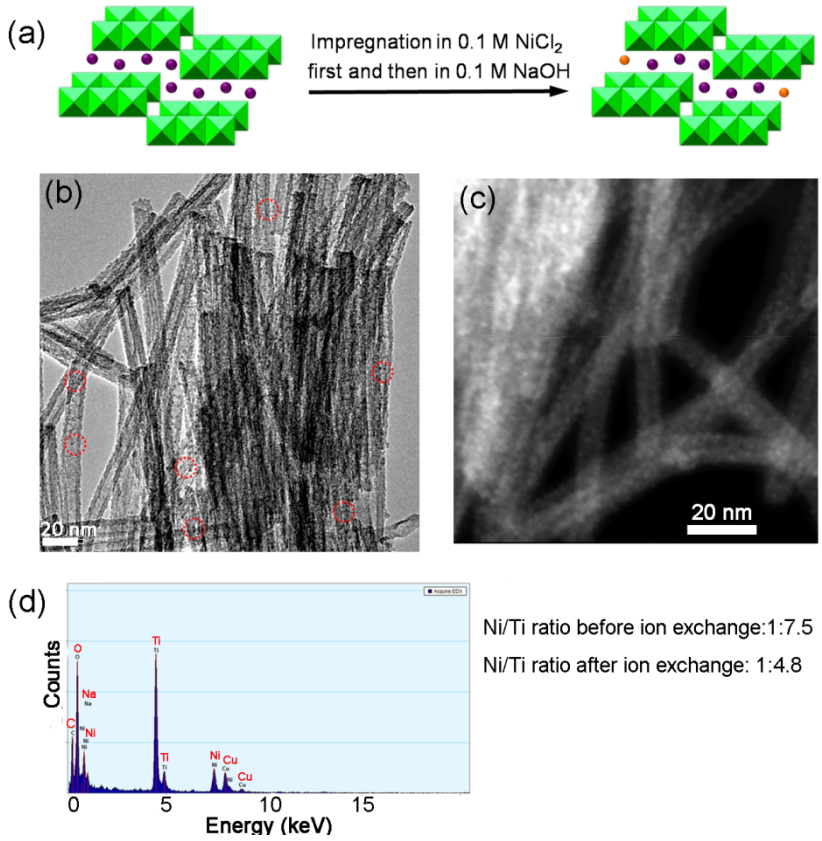

Fig. S15 (a) Diagrammatical description of the generation of more $Ni(OH)_2$ in the system of Ni^x/C/TNTs framework. Owing to the exchangeability of interlayer Na^+ in TNTs, Ni^{2+} ions can be introduced into TNTs readily and they can be precipitated into $Ni(OH)_2$ after the immersion in 0.1 M NaOH. (b) TEM and (c) high angle annular dark field scanning transmission electron microscopy (HAADF-STEM) images show the presence of tiny $Ni(OH)_2$ around the nanotubes after the above treatment, such as those marked by red circles. HAADF-STEM image intuitively reflect the bright dots corresponding to $Ni(OH)_2$ because the image contrast is roughly proportional to the square of the atomic number Z. In our system, the atomic number of Ni (Z=28) is larger than others (Ti: Z=22; Na: Z=11; O: Z=8; C: Z=6). (d) A typical EDS spectrum for Ni^x/C/TNTs framework, where the signal of Cu is attributed to copper grid for supporting the sample. Quantitative analysis based on EDS data revealed that Ni/Ti ratios was increased from the initial 1:7.5 to 1:4.8 after ion exchange treatment, which confirm the formation of more $Ni(OH)_2$.

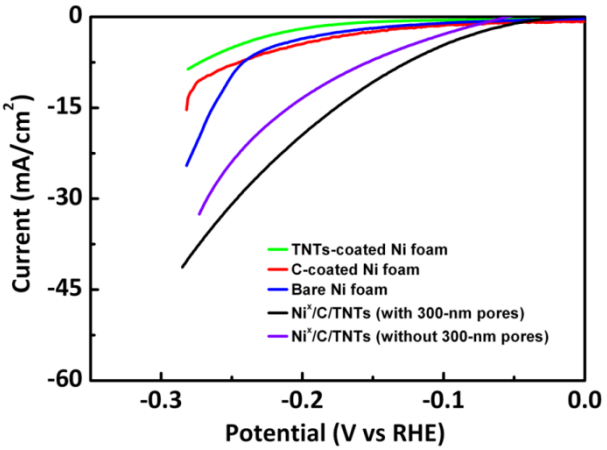

Fig. S16 A comparison among the HER performances of bare Ni foam (blue curve), C-coated Ni foam (red curve), single TNTs framework supported by the Ni foam (green curve), Ni^x/C/TNTs framework with the 300-nm pores (black curve), and Ni^x/C/TNTs framework without the 300-nm pores (violet curve).

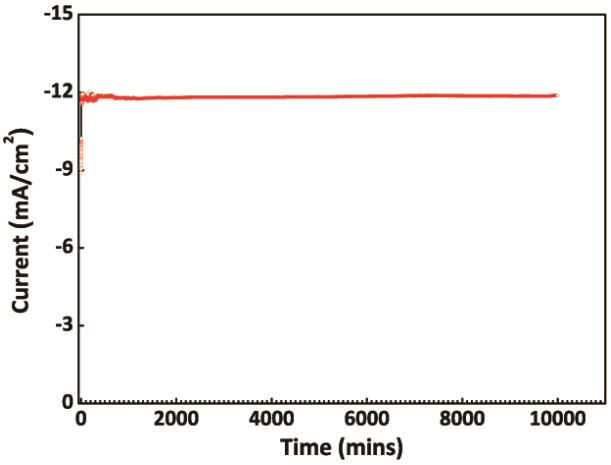

Fig. S17 Stability test of Ni^x/C/TNTs framework for HER. The 10000 mins of operation of the electrode demonstrates a little current attenuation, which manifests the ability of the Ni^x/C/TNTs framework in retaining the HER activity.

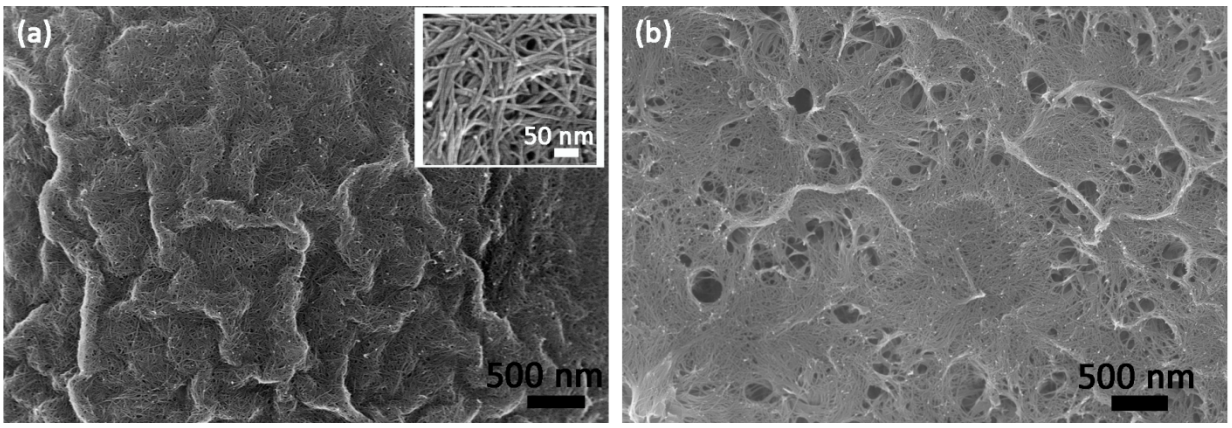

Fig. S18 A comparison between the Ni^x/C/TNTs framework without and with the 300 nm of pores. (a) SEM image of the reference Ni^x/C/TNTs framework (without the 300 nm of pores). Inset: A high-magnification SEM image shows the presence of the interstices among the nanotubes. (b) SEM image of the normal Ni^x/C/TNTs framework (with the 300 nm of pores). The reference Ni^x/C/TNTs framework was prepared without using the SiO_2 microspheres as the sacrificial templates, while the other conditions were kept identical to those for preparing the normal Ni^x/C/TNTs framework.

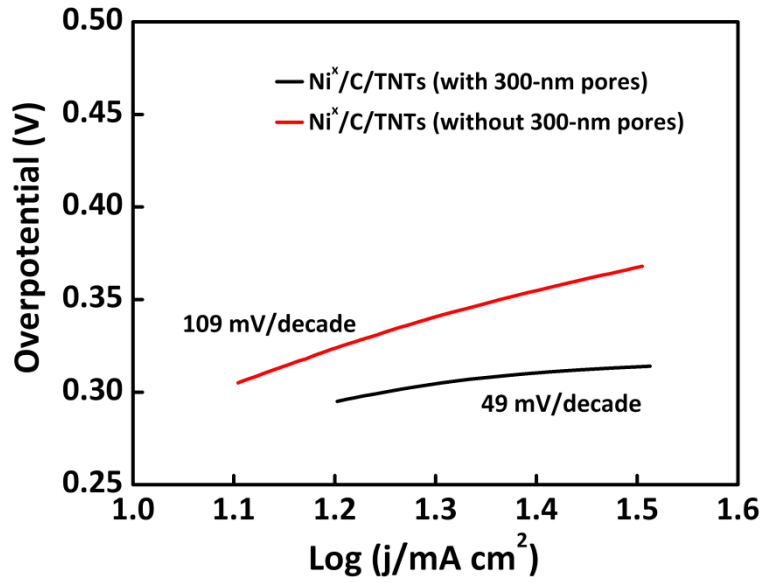

Fig. S19 Tafel plots for OER on Ni^x/C/TNTs framework with and without the 300-nm pores.

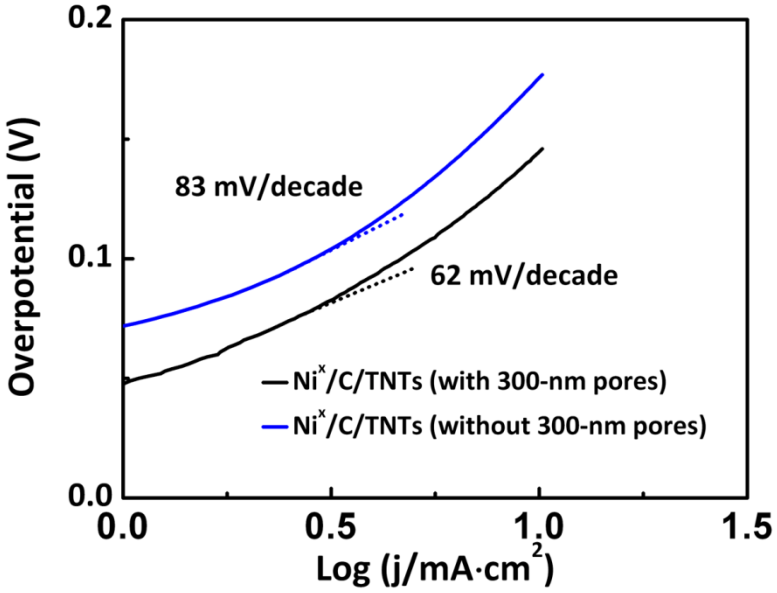

Fig. S20 Tafel plots for HER on Ni^x/C/TNTs framework with and without the 300-nm pores.

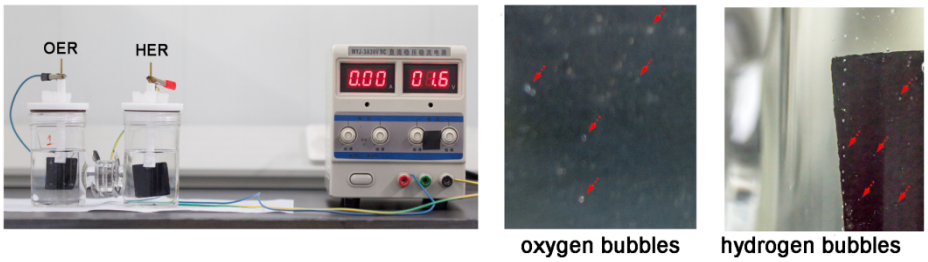

Fig. S21 Photographs showing the water-splitting device utilizing Ni^x/C/TNTs framework as both the cathode and the anode (left), the oxygen evolution (middle), and the hydrogen evolution (right). As denoted by arrows, abundant bubbles formed on both the anodic and cathodic Ni^x/C/TNTs framework at a small operating voltage of 1.6 V. The current is around 7 mA.